

Published in final edited form as:

*Mol Ther.* 2008 October ; 16(10): 1657–1664. doi:10.1038/mt.2008.163.

## Targeting mRNA Stability Arrests Inflammatory Bone Loss

Chetan S Patil<sup>1,2</sup>, Min Liu<sup>2</sup>, Wenpu Zhao<sup>2</sup>, Derek D Coatney<sup>2</sup>, Fei Li<sup>2</sup>, Elizabeth A VanTubergen<sup>2</sup>, Nisha J D'Silva<sup>2,3</sup>, and Keith L Kirkwood<sup>2</sup>

<sup>1</sup>Department of Oral Biology, State University of New York at Buffalo, Buffalo, New York, USA

<sup>2</sup>Department of Periodontics and Oral Medicine, University of Michigan, Ann Arbor, Michigan, USA

<sup>3</sup>Department of Pathology, University of Michigan, Ann Arbor, Michigan, USA

### Abstract

Many proinflammatory cytokines contain adenylate-uridylate-rich elements (AREs) within the 3'-untranslated region (UTR) that confer rapid mRNA destabilization. During the inflammatory response, cytokine mRNA are stabilized via complex interactions with RNA-binding proteins controlled by phosphorylation via multiple signaling pathways including the mitogen-activated protein kinases (MAPKs). In the absence of inflammation, a key cytokine-regulating RNA-binding protein, tristetraprolin (TTP), shuttles mRNA transcripts to degradation machinery in order to maintain low levels of inflammatory cytokines. Using this general model of mRNA decay, over expression of TTP was evaluated in an experimental model of inflammatory bone loss to determine whether altering cytokine mRNA stability has an impact in pathological bone resorption. Using adenoviral-delivered TTP, significant reductions of interleukin-6 (IL-6), tumor necrosis factor- $\alpha$  (TNF- $\alpha$ ), and prostaglandin (PG)E<sub>2</sub> were observed *in vitro* through a mechanism consistent with targeting mRNA stability. *In vivo* analysis indicates a significant protective effect from inflammation-induced bone loss and inflammatory infiltrate in animals overexpressing TTP compared with reporter controls. These findings provide experimental evidence that mRNA stability is a valid therapeutic target in inflammatory bone loss.

### INTRODUCTION

Inflammation-driven bone resorption results from the induction of inflammatory mediators through host response as exhibited in periodontal diseases. An important component of the pathobiology of periodontitis is sustained expression of proinflammatory cytokines because these mediators can directly or indirectly mediate osteoclastogenesis responsible for periodontal bone loss.<sup>1,2</sup> The nature and magnitude of the inflammatory infiltrate require stringent control over proinflammatory mediators. Such levels of control are achieved through multiple levels of gene regulation including induction and termination of transcriptional activation, mRNA processing and decay, and mRNA translation.<sup>3–5</sup>

The inflammatory response to Gram-negative periodontal pathogens requires activation of Toll-interleukin-1 receptor family members to initiate intracellular signaling. Multiple signaling cascades are stimulated during the inflammatory stress response including p38 mitogen-activated protein kinase (MAPK), jun N-terminal kinase (JNK), and nuclear factor- $\kappa$ B. Bacterial lipopolysaccharide (LPS) from periodontal pathogens *Porphyromonas gingivalis* and *Aggregatibacter actinomycetemcomitans* are capable of inducing cytokines such

© The American Society of Gene Therapy

**Correspondence:** Keith L. Kirkwood, Department of Microbiology and Immunology, Medical University of South Carolina, 173 Ashley Avenue, Charleston, South Carolina 29425, USA. E-mail: kkkirk@musc.edu.

as interleukin-6 (IL-6), IL-1, and tumor necrosis factor- $\alpha$  (TNF- $\alpha$ ) that are known to induce bone loss.<sup>2,3,6,7</sup> In human periodontitis, the levels of IL-6, TNF- $\alpha$ , and IL-2 $\beta$  are elevated<sup>8,9</sup> and produced by a variety of cells including gingival fibroblasts, macrophages, lymphocytes, and osteoblasts.<sup>10,11</sup> LPS additionally induces the production of nitric oxide, the free radical, and prostaglandin (PG)E<sub>2</sub> through the p38 MAPK pathway in human gingival fibroblasts.<sup>12</sup> Indeed, levels of PGE<sub>2</sub> induced by LPS stimulation have been associated with cyclooxygenase-2 (COX-2) levels and bone loss.<sup>13</sup>

The blockade of these cytokines *in vivo* has demonstrated the potent effects on bone metabolism and general health of animals.<sup>11,12,14</sup> The importance of cytokines in periodontal disease progression was demonstrated in nonhuman primates when specific antagonists of IL-1 and TNF- $\alpha$  inhibited the progression of bone loss in an experimental periodontitis model.<sup>14</sup> Additionally, in a ligature-induced periodontal model of bone loss in rats, meloxicam, a selective COX-2 inhibitor, was capable of inhibiting bone loss in rats.<sup>13</sup> More recently, inhibitors of p38 MAPK have been shown to prevent or arrest periodontal bone loss in experimental periodontitis models through selective inhibition of inflammatory cytokines including IL-6, TNF- $\alpha$ , and IL-1 $\beta$ .<sup>15,16</sup>

Cells of the immune system tightly regulate the production of potentially harmful cytokines by repressing their expression at the post-transcriptional level. The adenylate-uridylylate-rich elements (AREs), located in the 3'-untranslated region (UTR) of many cytokines (*e.g.*, granulocyte-macrophage colony-stimulating factor, TNF- $\alpha$ , IL-2, IL-3, IL-6) and other proinflammatory factors (*e.g.*, COX-2 and matrix metalloproteinase-13), play a major role in post-transcriptional repression. The presence of an ARE in a particular transcript can target it for rapid degradation or inhibit translation. p38 MAPK is a major signaling cascade implicated in facilitating stability of many proinflammatory cytokine mRNAs. AREs from 3'-UTRs of IL-6, IL-8, COX-2, and TNF- $\alpha$  mediate regulation of mRNA stability by p38 MAPK.<sup>17-21</sup>

These *cis*-acting ARE elements have been shown to affect stability of mRNA transcripts through interaction with RNA-binding proteins.<sup>17,22</sup> Proteins such as HuR have been associated with stabilizing transcripts. Upon shuttling to the cytoplasm, HuR binds ARE-containing transcripts and transports them to translational machinery. Alternatively, RNA-binding proteins such as tristetraprolin (TTP), and TTP-related proteins, butyrate response factor 1 and 2, have a major regulatory role in controlling cytokine mRNAs.<sup>23</sup> The TTP/butyrate response factor families of proteins bind to AREs with relatively high specificity through a characteristic zinc finger domain. The function of TTP was elucidated through several studies using TTP-deficient mice.<sup>24</sup> TTP<sup>-/-</sup> mice were shown to develop a generalized inflammatory condition, including an arthritic-like syndrome secondary to increased TNF- $\alpha$  and granulocyte-macrophage colony-stimulating factor levels.<sup>24</sup> In TTP<sup>-/-</sup> mice, the increased cytokine production was shown to be a result of increased mRNA stability.<sup>25,26</sup> TTP usually binds to mRNAs to promote rapid degradation by a mechanism whereby ARE transcripts are shuttled to exosomes.<sup>27</sup> However, during the inflammatory response once p38 MAPK pathway is activated, TTP is prevented from binding ARE mRNA after phosphorylated by p38 via its downstream kinase MAPK-activated protein kinase-2.<sup>17</sup>

In this study, an adenoviral-delivered TTP has been used as a therapeutic agent to inhibit ARE-containing cytokine expression and production. Using RNA stability as a target for gene therapy, LPS-induced bone loss has been arrested in an experimental periodontitis model. These data indicate that RNA stability functions *in vivo* for inflammation-induced bone loss and ARE-decay machinery may be a valid therapeutic target in inflammation-associated bone diseases.

## RESULTS

### Ad5-TTP selectively inhibits inflammatory mediators *in vitro*

To evaluate the effect of overexpressed TTP on ARE-containing cytokine expression and production, we transduced RAW264.7 macrophages with Ad5-TTP [600 multiplicity of infection (MOI)]. Preliminary immunoblot analysis of Ad5-TTP expression in RAW264.7 and HeLa cells indicated that optimal expression was achieved between 100 and 600 MOI in 24–36 h (data not shown). Enzyme-linked immunosorbent assay (ELISA) data in Figure 1 indicates that *A. actinomycetemcomitans* LPS is capable of potent stimulation of inflammatory mediators IL-6, TNF- $\alpha$ , and PGE<sub>2</sub>. Importantly, control viral particles expressing green fluorescent protein (GFP) did not inhibit LPS-induced cytokine production, while Ad5-TTP inhibited LPS-stimulated IL-6 ( $P < 0.001$ ), PGE<sub>2</sub> ( $P < 0.001$ ), and TNF- $\alpha$  ( $P < 0.001$ ) without any effect on non-stimulated cultures.

### Ad5-TTP decreases mRNA expression of key inflammatory mediators by targeting AREs

To determine whether overexpressed TTP could alter expression of inflammatory mediators at the level of mRNA, real-time reverse transcription-PCR was used to measure steady-state mRNA levels of COX-2, IL-6, and TNF- $\alpha$ . RAW264.7 macrophages were transduced with Ad5-GFP, Ad5-TTP, or without any viral particles and then stimulated with *A. actinomycetemcomitans* LPS (1  $\mu\text{g/ml}$ ) for 18 h. Total RNA was subject to real-time reverse transcription-PCR as described in the Materials and Methods section. In Figure 2a, cells that were untransduced or transduced with control viral particles expressing GFP showed significant induction of COX-2, IL-6, and TNF- $\alpha$  mRNA in response to LPS. However, macrophages transduced with TTP-expressing virus confirmed a significant inhibition of COX-2, IL-6, and TNF- $\alpha$  steady-state mRNA ( $P < 0.001$ ) to control culture levels (normalized to glyceraldehyde 3-phosphate dehydrogenase).

To further delineate the molecular targets of Ad5-TTP both ARE and non-ARE containing luciferase reporter expression was measured. HeLa cells were “adenofected” with Ad5-TTP or Ad5-GFP control virus along with luciferase reporters containing ARE of IL-6, TNF- $\alpha$ , COX-2 or non-ARE containing pGL3-control reporter plasmids (Figure 2b). After *A. actinomycetemcomitans* LPS stimulation, luciferase activity was determined from cell lysates. Nontransduced cells provided baseline levels of luciferase activity that was normalized to total protein. Cultures transduced with Ad5-GFP expressing ARE reporters resulted in luciferase activity that is not significantly different from nontransduced cells. Ad5-TTP adenofection significantly reduced IL-6 ARE ( $P < 0.05$ ), TNF- $\alpha$  ARE constitutive decay element ( $P < 0.01$ ), and COX-2 ARE ( $P < 0.001$ ). Importantly, control non-ARE reporter expression was not altered in GFP-or TTP-transduced cultures.

### *In vivo* optimization of Ad5 delivery

*In vivo* optimization of adenovirus expression through intraoral delivery was performed using an Ad5-luciferase reporter. Rats received intraperitoneal injections with luciferase substrate and luciferase activity was detected as described in the Materials and Methods section on days 1, 3, 7, 14, and 21 following a single intraoral injection of Ad5-luciferase. Representative bioluminescence activity from different MOIs at 7 days is shown in Figure 3a. High levels of luciferase activity were readily detected through 21-days end point when 500 and 1,000 MOI of adenovirus was used (Figure 3b). Animals from 100 and 10,000 MOI groups were reinfected with adenovirus to evaluate expression. These animals did not express luciferase activity (data not shown).

### Adenoviral delivered TTP is expressed through the experimental protocol in periodontal tissues

Figure 4 shows *in vivo* TTP expression after Ad5-GFP and Ad5-TTP transduction of periodontal tissues. Using sections following the experimental period, control and Ad5-TTP tissues were immunostained from TTP. Immunoglobulin G isotype controls showed little background staining after extensive optimization (data not shown). Data from these studies indicate that Ad5-TTP is strongly expressed in injected areas (Figure 4e) but not from adjacent areas (Figure 4f) or Ad5-GFP-transduced tissues (Figure 4b and c shown at high magnification).

### Adenoviral-delivered TTP prevents experimental periodontitis

Figure 5a illustrates representative microcomputed tomography ( $\mu$ CT)-scanned data that was re-formatted to generate a three-dimensional image of the rat hemi-maxillae in each treatment group. Using the compiled data, bone loss was measured using linear and volumetric analysis. Linear analysis measured in millimeters (mm) between the cemento-enamel junction and the alveolar bone crest. Figure 5b indicates *A. actinomycetemcomitans* LPS delivery in nontransduced and Ad5-GFP transduced rats resulted in significant linear bone loss ( $P < 0.05$ ). Ad5-TTP-transduced animals displayed similar levels of bone height when compared with phosphate-buffered saline (PBS)-injected animals. *A. actinomycetemcomitans* LPS injections in Ad5-TTP-transduced animals displayed extensive protection from linear bone loss compared with LPS-treated animals ( $P < 0.01$ ). To eliminate any linear measurement basis, bone volume analysis was used to determine whether Ad5-TTP had a significant effect to preserve bone levels in this animal model of bone destruction as recently described.<sup>15,16,28</sup> As shown in Figure 5c, bone volume levels from PBS-injected GFP and TTP-expressing rats are not significantly different. In animals injected with LPS, nontransduced and Ad5-GFP-transduced animals show substantial bone volume loss ( $P < 0.05$ ). Ad5-TTP-transduced rats did not demonstrate significant bone volume loss when injected with *A. actinomycetemcomitans* LPS compared with nontransduced and Ad5-GFP-transduced animals ( $P < 0.01$ ).

### Ad5-TTP decreases inflammatory infiltrate and osteoclast recruitment

To examine intraoral tissues from rats locally expressing TTP or control virus, histological sections were evaluated to enumerate inflammatory cells and osteoclasts. Histological analysis between first and second molar demonstrated low levels of neutrophils, macrophages, and lymphocytes in all PBS-injected animals regardless of viral transduction (Figure 6 and Table 1). The presence of inflammatory cells increased considerably in LPS-injected tissue. In Ad5-GFP and Ad5-TTP-transduced tissues, slight elevation of inflammatory cells was observed. These data are consistent with the ability of the immunocompetent animal to generate an immune response to the adenovirus. In animals injected with LPS in the presence of Ad5-TTP, the levels of inflammatory cell counts were reduced to those observed in PBS-injected animals. Tissue sections were also subjected to tartate-resistant acid phosphatase (TRAP) staining (Figure 7). TRAP<sup>+</sup> cells were visually enumerated between maxillary first and second molars. PBS-injected animals had baseline levels of TRAP expression for nontransduced and transduced animals. *A. actinomycetemcomitans* LPS-injected animals resulted in dramatically greater number of TRAP<sup>+</sup> cells in nontransduced and Ad5-GFP-transduced animals ( $P < 0.001$ ). Ad5-TTP infection prevented LPS-induced increase in osteoclast formation.

## DISCUSSION

TTP deficiency is associated with cachexia, arthritis, and autoimmunity, resulting from increasing ARE inflammatory cytokine production.<sup>24,25</sup> Many studies have evaluated the overexpression of TTP on exogenous ARE reporters *in vitro*.<sup>29–32</sup> We have demonstrated in

a proof-of-principle model system that overexpression of TTP decreases endogenous ARE cytokine levels *in vitro* and protects from inflammation-induced bone loss *in vivo*.

Activation of the p38/MAPK-activated protein kinase-2 pathway through LPS binding results in the phosphorylation of TTP at serine 52 and 178 (ref. <sup>33</sup>). This phosphorylation sequesters TTP with 14:3:3 and inhibits interaction of TTP with ARE mRNA.<sup>34</sup> Thus, ARE mRNAs are spared from TTP shuttling to degradation machinery and are given an opportunity for translation.<sup>35,36</sup> Once the inflammatory stimulus is resolved, TTP becomes hypophosphorylated<sup>37</sup> permitting interaction of TTP with ARE mRNA once again to facilitate decay of the mRNA at P-bodies and exosomes.<sup>23,32</sup>

The regulation of TTP occurs as a result of mRNA and protein stability through MAPK pathways. Interestingly, LPS stimulation induces TTP gene expression<sup>25,38</sup> that is regulated by TTP protein through the p38 MAPK pathway as described above.<sup>30</sup> Upon LPS stimulation, multiple pathways are activated, including JNK, extracellular signal-regulated kinase, and p38 MAPK.<sup>6,39</sup> Over activation of p38 MAPK and extracellular signal-regulated kinase results in a synergistic stabilization of TNF- $\alpha$  reporter constructs.<sup>40</sup> Mechanistically, pharmacological inhibition of p38 MAPK results in TTP localization to the nucleus, an effect that is synergized by the inhibition of extracellular signal-regulated kinase.<sup>39</sup> It is believed that TTP protein undergoes degradation after nuclear localization.<sup>39</sup> However, not all groups have observed this nuclear localization, thus nuclear localization may not be a pre-requisite for degradation.<sup>38</sup>

Ultimately, activated p38 MAPK stabilizes TTP protein by preventing degradation via 20/26 proteasome.<sup>39</sup> Further evidence suggests that stabilization through the p38 MAPK pathway may result from phosphorylation of sites alternative to serine 52 and 178 refs. <sup>37,38</sup>. Experimentation involving the over activation of JNK pathways has demonstrated the rapid inhibition of p38 MAPK-mediated stability. Although the mechanism has not been clearly defined, it is believed that JNK activation increases the expression of dual specificity kinases that dephosphorylate and inactivate p38 MAPK. This notion is additionally supported by the observation of hyperphosphorylated p38 MAPK when JNK is pharmacologically inhibited.<sup>40,41</sup> Thus it is clear that multiple MAPK pathways have direct and indirect input in the regulation of mRNA stability. This complicates the function of TTP in RNA stability and has led us to the question of whether overexpressed TTP could functionally inhibit ARE proinflammatory cytokines.

To prevent Ad5-TTP self-regulation, we used an expression construct containing a cytomegalovirus promoter along with the TTP-coding sequence but lacking the TTP 3'-UTR. Although this circumvents regulation via mRNA stability, TTP is still capable of being regulated by post-translational mechanisms involving MAPK pathways.<sup>39</sup> Using this adenoviral delivery system, we have demonstrated that TTP overexpression can significantly reduce protein secretion of IL-6, TNF- $\alpha$ , and PGE<sub>2</sub> as detected using ELISA in macrophages. Although efforts have been made to demonstrate the involvement of endogenous TTP regulation of IL-6 mRNA stability, these studies have only used reporter systems or evaluated the end-result of protein production.<sup>42,43</sup> While we have not evaluated this interaction, our data supports that TTP overexpression reduces IL-6. Ongoing studies are addressing mechanisms of IL-6 ARE regulation by TTP (unpublished data). The levels of protein reduction vary among the inflammatory mediators (PGE<sub>2</sub> and TNF- $\alpha$  reduced by ~50%, IL-6 reduced by ~85%; Figure 1a). As measured by real-time reverse transcription PCR, steady-state mRNA levels of COX-2, IL-6, and TNF- $\alpha$  were reduced near baseline levels (Figure 1b). Because COX-2 protein levels were not directly measured, we cannot rule out that COX-2 protein was abolished. However, data available from several studies suggest that COX-2 and PGE<sub>2</sub> levels are correlated *in vitro* and *in vivo*.<sup>44,45</sup> Additional data suggests endotoxin-induced PGE<sub>2</sub> may not be accounted for COX-1 activity.<sup>46</sup>

This study used cell lines from different species confirming a conserved role for TTP in reducing class II ARE mRNA levels (Figure 1 and Figure 2). *In vitro* endogenous steady-state mRNA data combined with ELISA and ARE reporter assay data provide significant evidence that TTP inhibits endogenous and exogenous ARE mRNA. These data are consistent with the literature where TTP is overexpressed.<sup>18,31,36</sup> Interestingly, we were not able to detect consistent changes in endogenous mRNA stability in our model of TTP overexpression (data not shown). The model system we used maintained very (basal) low levels of mRNA similar to unstimulated cells. This, in part, made it difficult to show a consistent reduction in mRNA stability.

The primary end point in these studies is periodontal bone loss. Analysis of  $\mu$ CT data from hemi-maxillae initially used linear measurement that is analogous to clinical examination in humans (Figure 5b). In order to verify these linear data, volume analysis was used to determine whether Ad5-TTP had a protective effect on inflammatory bone loss (Figure 5c).

The presence of inflammatory cells is very high in LPS-injected animals (Figure 6). Although there are few inflammatory cells detected within the Ad5-GFP-infected animals, the intensity of inflammatory infiltrate is greater than those of LPS-injected animals. Importantly, the number of inflammatory cells in Ad5-TTP-transduced animals was at baseline levels for PBS- and LPS-injected animals suggesting a reduced inflammatory response. When evaluating TRAP-positive cells in tissue sections, Ad-GFP and nontransduced animals injected with LPS demonstrated high TRAP-positive cell counts. Animals overexpressing TTP presented with TRAP-positive cell numbers similar to PBS-injected animals regardless of LPS injection (Figure 7). The production of proinflammatory cytokines has been well correlated with inflammatory periodontal bone loss resulting from osteoclast differentiation and activation.<sup>14,28,47,48</sup> This trend is similar to that observed when evaluating inflammatory cells counts. This correlation suggests an inability of LPS to cause inflammation-induced bone loss in animals overexpressing TTP.

Although TTP overexpression has been shown to mediate effects through *in vitro* studies using ARE reporters, these studies are the first to evaluate TTP as a therapeutic agent *in vivo*. Multiple MAPK pathways are activated upon LPS stimulation that induce proinflammatory cytokine gene expression. After p38/MAPK-activated protein kinase-2 phosphorylation of TTP, ARE mRNA does not retain TTP which permits shuttling to translational machinery, enhancing cytokine production. However, in an overexpression setting, TTP is present in abundance at the time of LPS stimulation. Thus, despite MAPK pathway activation not all TTP will be phosphorylated, allowing nonphosphorylated TTP to engage ARE-containing mRNA. This interaction allows for the shuttling of ARE mRNA to degradation components resulting in a net reduction of ARE-containing cytokine production. Ongoing studies are addressing the potential of TTP to function in an infectious model of periodontitis. These studies indicate that in a preventive model of experimental periodontitis, mRNA stability regulation plays a major role in LPS-induced inflammatory bone loss. However, in human periodontal pathology, infectious bacteria are capable of interacting with the host. Although LPS is a potent inflammatory mediator, there are other components within live organisms that can induce apoptosis, modulate the immune response, and evade the immune response. Further investigation using live infection models would be necessary to ascertain the truly protective benefits of this preventive therapeutic approach.

Although there are several steps required to use TTP as a therapeutic, these data suggest that this RNA-binding protein can function as an anti-inflammatory therapeutic in an LPS-induced inflammatory bone loss model.

## MATERIALS AND METHODS

### Cells and materials

HeLa (ATCC CCL 2) cervical cancer and RAW264.7 (ATCC TIB-71) monocyte/macrophage cell lines were obtained from American Type Cell Collection (Manassas, VA). All cells were cultured with Dulbecco's modified Eagle's media (Invitrogen, Carlsbad, CA) supplemented with 10% heat-inactivated fetal bovine serum, 100 IU/ml penicillin, 100 µg/ml streptomycin in a 37 °C incubator containing 5% CO<sub>2</sub>. *A. actinomycetemcomitans* LPS serotype b was purified and characterized from strain Y4 as described previously.<sup>28</sup> ARE reporter plasmids were constructed through PCR cloning into pGL3-control (Promega, Madison, WI) vector containing the luciferase reporter gene. IL-6 3'-UTR (1–403) was amplified from the mIL-6 complementary DNA in pCR2.1 by PCR using primers terminating in *Xba*I recognition sequences: forward, 5'-CCTCTAGATAGTGCGTTATGCCTAAGCA-3'; reverse, 5'-CCTCTAGAGTTTGAAGACAGTCTAAACAT-3' and were ligated in the unique *Xba*I site of the pGL3-control vector (Promega). TNF-α constitutive decay element corresponding to 3'-UTR (received as gift for [confirm] pTet-7B-TNFCDE from P. Anderson, Harvard University) was PCR amplified and ligated cloned into *Xba*I site of pGL3-control using primers terminating in *Xba*I recognition sequences: forward: 5'-TTTTCTAGA-GGAAGGCCGGGGTGT-3'; reverse 5'-TTTTCTAGACTCAGCTCCGTTTTACAGA-3'. The COX-2 ARE reporter was received in pGL3-control as a gift from A. Morrison (Washington University). All ARE reporters were sequenced to verify authenticity before use.

### Viral generation, transduction, and adenofection

DLE3 replication-deficient adenovirus expressing GFP and TTP were generated through the Vector Core at University of Michigan (Thomas Lanigan, Director). Serotype-5 adenovirus containing human TTP was generated by excising the coding sequence from FLAG-TTP (gift from Jens Lykke-Anderson) and subcloning into the pACCMV2 shuttle vector. Through LOX-P integration, the TTP-coding sequence was integrated into the adenoviral expression construct. Viral particle production and titer was performed in human retina cell line HER911.

### ELISA

RAW264.7 cells were plated at  $5 \times 10^4$  cells/well in 24-well dishes and then infected with Ad5-GFP or Ad5-TTP for 12 hours. Cells were then stimulated with *A. actinomycetemcomitans* LPS (1 µg/ml) for an additional 24 hours. Vehicle-only cultures served as controls. Cell culture supernatants were harvested and IL-6, TNF-α, and PGE<sub>2</sub> levels were analyzed using ELISA according to manufacturer's instructions (R&D Systems, Minneapolis, MN).

### Real-time reverse transcription PCR

Total RNA was isolated from control and transduced cells as described above using TRIZOL (Invitrogen) according to the manufacturer's instructions and quantitated via spectrophotometer. Complementary DNA was synthesized by a reverse transcription kit (Applied Biosystems, Foster City, CA) using 300 ng total RNA in a 15-µl reaction. PCR thermocycler (Applied Biosystems 7500 Real-Time PCR System) conditions used were as follows: 50 °C for 2 minutes, 95 °C for 10 minutes, and 50 cycles of 95 °C for 15 seconds, 60 °C for 1 minute. Amplicon primers were obtained through Assays on Demand (Applied Biosystems, Foster City, CA) for murine IL-6 (Mm00446190\_m1), TNF-α (Mm00443258\_m1), COX-2 (Mm00478374\_m1), and glyceraldehydes 3-phosphate dehydrogenase (Mm99999915\_g1). Amplicon concentration was determined using threshold cycle values compared with standard curves for each primer. IL-6, TNF-α, and COX-2 mRNA

levels were quantitated, normalized to glyceraldehyde 3-phosphate dehydrogenase, and expressed as fold change compared with control cultures.

### ARE reporter gene assays

Adenoviral transduction was used to attain high ectopic gene expression *in vitro* and *in vivo*. HeLa cells were transduced with Ad5-TTP or Ad-5-GFP control viral particles at 600 MOI. After 3 hours, serum was added to cells and media was refreshed 12 hours after transduction. For ARE reporter assays, cells were subsequently transfected with ARE reporter plasmids for IL-6, TNF- $\alpha$ , COX-2 [according to protocol using Lipofectamine PLUS (Invitrogen)]. Twelve hours after transfection, cells were stimulated with *A. actinomycetemcomitans* LPS (1  $\mu$ g/ml) for 24 hours. Cells lysates were harvested and subjected to luciferase activity assays (Dual luciferase Assay, Promega) and luciferase activity measured using luminometer (LMaxII, Molecular Devices, Sunnyvale, CA).

### In vivo bioluminescence imaging

To determine the *in vivo* dose for intraoral application of Ad5-TTP, an Ad5-luciferase reporter virus was used to monitor MOI and time optimization. Bioluminescence was performed following one-time injection of Ad5-luciferase at indicated MOIs ( $n = 3$ /group). Bioluminescence activity was measured on days 1, 3, 7, 14, and 21 after injection via a cryogenically cooled imaging system (Xenogen, Alameda, CA). Before imaging, animals were anesthetized in an acrylic chamber with 1.5% isoflurane/air mixture and injected intraperitoneally with 40 mg/ml of luciferin potassium salt in PBS at a dose of 150 mg/kg body weight as previously described.<sup>49,50</sup> The University Committee on the Use and Care of Animals at the University of Michigan approved all protocols.

### Experimental periodontitis model

Twenty-four female adult Sprague-Dawley rats (~250 g) were housed under specific pathogen-free conditions in pairs with food and tap water *ad libitum*. Once weekly, animals were weighed to ensure proper growth and nutrition. Rats were injected one time in the palatal region between the maxillary first and second molars with no adenovirus ( $n = 8$ ), adenovirus expressing GFP ( $1 \times 10^9$  plaque-forming units in 4  $\mu$ l total volume;  $n = 8$ ), or adenovirus expressing TTP ( $1 \times 10^9$  plaque-forming units in 8  $\mu$ l total volume;  $n = 8$ ) at day 0. Twenty-four hours after adenoviral delivery, rats were subdivided so that half of the groups ( $n = 4$ ; eight hemi-maxillas) received either *A. actinomycetemcomitans* LPS (6  $\mu$ l of a 10 mg/ml) delivered bilaterally to the palatal gingival tissue via a 33-gauge Hamilton syringe between the maxillary first and second molars three times per week for 4 weeks (144  $\mu$ g of LPS/animal over the 4-week period), or mock injection control PBS delivered bilaterally between the first and second molars three times per week for 4 weeks PBS as recently described.<sup>16</sup> At the end of the experimental period, animals were killed, maxillas hemisected ( $n = 8$ /group) and posterior block sections were immersed directly in 10% buffered formalin fixative solution.

### Microcomputed tomography

Nondemineralized rat maxillae ( $n=8$ /group) were scanned by a cone beam  $\mu$ CT system (GE Healthcare BioSciences, Chalfont St. Giles, UK) as previously described.<sup>15</sup> Each scan was reconstructed at a mesh size of  $18 \times 18 \times 18 \mu\text{m}$ , and three-dimensional digitized images were generated for each specimen. Using GEHC MicroView software (version viz. + 2.0 build 0029), the images were rotated into a standard orientation and threshold to distinguish between mineralized and nonmineralized tissue. For each specimen, a grayscale voxel value histogram was generated to determine an optimal threshold value. Linear measurements on bone loss were taken from cemento-enamel junction to alveolar bone crest and volume of bone loss were measured as described.<sup>15,16</sup> Examiners (D.D.C. and C.P.) were trained at the University of



Michigan Core Center for Musculoskeletal Disorders where all  $\mu$ CT scans were measured in a blinded manner.

### Histology, immunohistochemistry, and TRAP staining

Formalin-fixed specimens were decalcified in a 10% EDTA solution for 2 weeks at 4 °C. The maxillas were paraffin embedded, and sagittal sections (5  $\mu$ m) were prepared. Some sections were stained with hematoxylin and eosin for descriptive histology. Immunohistochemical staining was performed as described previously.<sup>15</sup> Antigen retrieval was performed with sodium citrate buffer (10 mmol/l, pH 6, 95 °C). Tissue sections were incubated with rabbit anti-TTP polyclonal antibody (3  $\mu$ g/ml, Abcam, Cambridge, MA) for 1 hour at room temperature. Subsequently, tissue sections were incubated with biotinylated donkey anti-rabbit Immunoglobulin G (Biocare Medical, Walnut Creek, CA) and biotin–streptavidin conjugated to peroxidase. The chromogen DAB 500 was used for immunodetection. Images were captured using an inverted scope (Nikon TS100) and mega pixel camera (Nikon CCD camera with 5.1). For enumeration of osteoclasts, TRAP staining was performed on a representative slide from each treatment group using a leukocyte acid phosphatase kit (Sigma, St Louis, MO). Active osteoclasts were defined as multinucleated TRAP-positive cells in contact with the bone surface as described.<sup>28</sup> Slides from approximately the same sagittal sections were used to enumerate TRAP-positive cells.

### Statistical analysis

All data were subject to statistical analysis through appropriate analysis parameters. Two-way analysis of variance was used when multifactorial statistical analysis was needed. Two-way analysis of variance with Bonferroni post-tests was performed using Graphpad Prism (version 4.03) Graphpad Software (San Diego, CA).

## ACKNOWLEDGMENTS

We acknowledge the Vector Core (Thomas Lanigan, Director) and the Musculoskeletal Core (Steven Goldstein, Director) at the University of Michigan. These studies were supported by grants NIH DE017966, DE018290, and Department of Defense W81XWH-05-1-0075. This work was conducted in Ann Arbor, Michigan, USA.

## REFERENCES

1. Teng YT. The role of acquired immunity and periodontal disease progression. *Crit Rev Oral Biol Med* 2003;14:237–252. [PubMed: 12907693]
2. Teng YT. Mixed periodontal Th1-Th2 cytokine profile in *Actinobacillus actinomycetemcomitans*-specific osteoprotegerin ligand (or RANK-L)-mediated alveolar bone destruction *in vivo*. *Infect Immun* 2002;70:5269–5273. [PubMed: 12183580]
3. Patil CS, Kirkwood KL. p38 MAPK signaling in oral-related diseases. *J Dent Res* 2007;86:812–825. [PubMed: 17720848]
4. Hamilton TA, Novotny M, Datta S, Mandal P, Hartupee J, Tebo J, et al. Chemokine and chemoattractant receptor expression: post-transcriptional regulation. *J Leukoc Biol* 2007;82:213–219. [PubMed: 17409125]
5. Hamilton TA, Ohmori Y, Tebo J. Regulation of chemokine expression by antiinflammatory cytokines. *Immunol Res* 2002;25:229–245. [PubMed: 12018462]
6. Patil C, Rossa C Jr, Kirkwood KL. *Actinobacillus actinomycetemcomitans* lipopolysaccharide induces interleukin-6 expression through multiple mitogen-activated protein kinase pathways in periodontal ligament fibroblasts. *Oral Microbiol Immunol* 2006;21:392–398. [PubMed: 17064398]
7. Rossa C, Ehmann K, Liu M, Patil C, Kirkwood KL. MKK3/6-p38 MAPK signaling is required for IL-1 $\beta$  and TNF- $\alpha$ -induced RANKL expression in bone marrow stromal cells. *J Interferon Cytokine Res* 2006;26:719–729. [PubMed: 17032166]

8. Hirose K, Isogai E, Miura H, Ueda I. Levels of *Porphyromonas gingivalis* Fimbriae and inflammatory cytokines in gingival crevicular fluid from adult human subjects. *Microbiol Immunol* 1997;41:21–26. [PubMed: 9087964]
9. Geivelis M, Turner DW, Pederson ED, Lamberts BL. Measurements of interleukin-6 in gingival crevicular fluid from adults with destructive periodontal disease. *J Periodontol* 1993;64:980–983. [PubMed: 8277408]
10. Takeichi O, Saito I, Tsurumachi T, Moro I, Saito T. Expression of inflammatory cytokine genes *in vivo* by human alveolar bone-derived polymorphonuclear leukocytes isolated from chronically inflamed sites of bone resorption. *Calcif Tissue Int* 1996;58:244–248. [PubMed: 8661955]
11. Takeichi O, Saito I, Tsurumachi T, Saito T, Moro I. Human polymorphonuclear leukocytes derived from chronically inflamed tissue express inflammatory cytokines *in vivo*. *Cell Immunol* 1994;156:296–309. [PubMed: 8025949]
12. Gutierrez-Venegas G, Maldonado-Frias S, Ontiveros-Granados A, Kawasaki-Cardenas P. Role of p38 in nitric oxide synthase and cyclooxygenase expression, and nitric oxide and PGE2 synthesis in human gingival fibroblasts stimulated with lipopolysaccharides. *Life Sci* 2005;77:60–73. [PubMed: 15848219]
13. Nassar CA, Nassar PO, Nassar PM, Spolidorio LC. Selective cyclooxygenase-2 inhibition prevents bone resorption. *Braz Oral Res* 2005;19:36–40. [PubMed: 16229354]
14. Assuma R, Oates T, Cochran D, Amar S, Graves DT. IL-1 and TNF antagonists inhibit the inflammatory response and bone loss in experimental periodontitis. *J Immunol* 1998;160:403–409. [PubMed: 9551997]
15. Kirkwood KL, Li F, Rogers JE, Otremba J, Coatney DD, Kreider JM, et al. A p38alpha selective mitogen-activated protein kinase inhibitor prevents periodontal bone loss. *J Pharmacol Exp Ther* 2007;320:56–63. [PubMed: 17041006]
16. Rogers JE, Li F, Coatney DD, Otremba J, Kriegl JM, Protter TA, et al. A p38 mitogen-activated protein kinase inhibitor arrests active alveolar bone loss in a rat periodontitis model. *J Periodontol* 2007;78:1992–1998. [PubMed: 18062121]
17. Mahtani KR, Brook M, Dean JL, Sully G, Saklatvala J, Clark AR. Mitogen-activated protein kinase p38 controls the expression and posttranslational modification of tristetraprolin, a regulator of tumor necrosis factor alpha mRNA stability. *Mol Cell Biol* 2001;21:6461–6469. [PubMed: 11533235]
18. Stoecklin G, Stoeckle P, Lu M, Muehlemann O, Moroni C. Cellular mutants define a common mRNA degradation pathway targeting cytokine AU-rich elements. *RNA* 2001;7:1578–1588. [PubMed: 11720287]
19. Kotlyarov A, Neininger A, Schubert C, Eckert R, Birchmeier C, Volk HD, et al. MAPKAP kinase 2 is essential for LPS-induced TNF-alpha biosynthesis. *Nat Cell Biol* 1999;1:94–97. [PubMed: 10559880]
20. Neininger A, Kontoyiannis D, Kotlyarov A, Winzen R, Eckert R, Volk HD, et al. MK2 targets AU-rich elements and regulates biosynthesis of tumor necrosis factor and interleukin-6 independently at different post-transcriptional levels. *J Biol Chem* 2002;277:3065–3068. [PubMed: 11741878]
21. Winzen R, Kracht M, Ritter B, Wilhelm A, Chen CY, Shyu AB, et al. The p38 MAP kinase pathway signals for cytokine-induced mRNA stabilization via MAP kinase-activated protein kinase 2 and an AU-rich region-targeted mechanism. *EMBO J* 1999;18:4969–4980. [PubMed: 10487749]
22. Wang JG, Collinge M, Ramgolam V, et al. LFA-1-dependent HuR nuclear export and cytokine mRNA stabilization in T cell activation. *J Immunol* 2006;176:2105–2113. [PubMed: 16455966]
23. Varnum BC, Ma QF, Chi TH, Fletcher B, Herschman HR. The TIS11 primary response gene is a member of a gene family that encodes proteins with a highly conserved sequence containing an unusual Cys-His repeat. *Mol Cell Biol* 1991;11:1754–1758. [PubMed: 1996120]
24. Taylor GA, Carballo E, Lee DM, Lai WS, Thompson MJ, Patel DD, et al. A pathogenetic role for TNF alpha in the syndrome of cachexia, arthritis, and autoimmunity resulting from tristetraprolin (TTP) deficiency. *Immunity* 1996;4:445–454. [PubMed: 8630730]
25. Carballo E, Lai WS, Blackshear PJ. Feedback inhibition of macrophage tumor necrosis factor-alpha production by tristetraprolin. *Science* 1998;281:1001–1005. [PubMed: 9703499]

26. Carballo E, Lai WS, Blackshear PJ. Evidence that tristetraprolin is a physiological regulator of granulocyte-macrophage colony-stimulating factor messenger RNA deadenylation and stability. *Blood* 2000;95:1891–1899. [PubMed: 10706852]
27. Rigby WF, Roy K, Collins J, Rigby S, Connolly JE, Bloch DB, et al. Structure/function analysis of tristetraprolin (TTP): p38 stress-activated protein kinase and lipopolysaccharide stimulation do not alter TTP function. *J Immunol* 2005;174:7883–7893. [PubMed: 15944294]
28. Rogers JE, Li F, Coatney DD, Rossa C, Bronson P, Krieder JM, et al. *Actinobacillus actinomycetemcomitans* lipopolysaccharide-mediated experimental bone loss model for aggressive periodontitis. *J Periodontol* 2007;78:550–558. [PubMed: 17335380]
29. Blackshear PJ, Lai WS, Kennington EA, Brewer G, Wilson GM, Guan X, et al. Characteristics of the interaction of a synthetic human tristetraprolin tandem zinc finger peptide with AU-rich element-containing RNA substrates. *J Biol Chem* 2003;278:19947–19955. [PubMed: 12639954]
30. Tchen CR, Brook M, Saklatvala J, Clark AR. The stability of tristetraprolin mRNA is regulated by mitogen-activated protein kinase p38 and by tristetraprolin itself. *J Biol Chem* 2004;279:32393–32400. [PubMed: 15187092]
31. Boutaud O, Dixon DA, Oates JA, Sawaoka H. Tristetraprolin binds to the COX-2 mRNA 3' untranslated region in cancer cells. *Adv Exp Med Biol* 2003;525:157–160. [PubMed: 12751757]
32. Hau HH, Walsh RJ, Ogilvie RL, Williams DA, Reilly CS, Bohjanen PR. Tristetraprolin recruits functional mRNA decay complexes to ARE sequences. *J Cell Biochem* 2007;100:1477–1492. [PubMed: 17133347]
33. Chrestensen CA, Schroeder MJ, Shabanowitz J, Hunt DF, Pelo JW, Worthington MT, et al. MAPKAP kinase 2 phosphorylates tristetraprolin on *in vivo* sites including Ser178, a site required for 14-3-3 binding. *J Biol Chem* 2004;279:10176–10184. [PubMed: 14688255]
34. Stoecklin G, Stubbs T, Kedersha N, Wax S, Rigby WF, Blackwell TK, et al. MK2-induced tristetraprolin:14-3-3 complexes prevent stress granule association and ARE-mRNA decay. *EMBO J* 2004;23:1313–1324. [PubMed: 15014438]
35. Stoecklin G, Mayo T, Anderson P. ARE-mRNA degradation requires the 5'-3' decay pathway. *EMBO Rep* 2006;7:72–77. [PubMed: 16299471]
36. Lai WS, Carballo E, Strum JR, Kennington EA, Phillips RS, Blackshear PJ. Evidence that tristetraprolin binds to AU-rich elements and promotes the deadenylation and destabilization of tumor necrosis factor alpha mRNA. *Mol Cell Biol* 1999;19:4311–4323. [PubMed: 10330172]
37. Sun L, Stoecklin G, Van Way S, Hinkovska-Galcheva V, Guo RF, Anderson P, et al. Tristetraprolin (TTP)-14-3-3 complex formation protects TTP from dephosphorylation by protein phosphatase 2a and stabilizes tumor necrosis factor-alpha mRNA. *J Biol Chem* 2007;282:3766–3777. [PubMed: 17170118]
38. Fairhurst AM, Connolly JE, Hintz KA, Goulding NJ, Rassias AJ, Yeager MP, et al. Regulation and localization of endogenous human tristetraprolin. *Arthritis Res Ther* 2003;5:R214–R225. [PubMed: 12823857]
39. Brook M, Tchen CR, Santalucia T, McIlrath J, Arthur JS, Saklatvala J, et al. Posttranslational regulation of tristetraprolin subcellular localization and protein stability by p38 mitogen-activated protein kinase and extracellular signal-regulated kinase pathways. *Mol Cell Biol* 2006;26:2408–2418. [PubMed: 16508015]
40. Deleault KM, Skinner SJ, Brooks SA. Tristetraprolin regulates TNF TNF-alpha mRNA stability via a proteasome dependent mechanism involving the combined action of the ERK and p38 pathways. *Mol Immunol* 2008;45:13–24. [PubMed: 17606294]
41. Lang R, Hammer M, Mages J. DUSP meet immunology: dual specificity MAPK phosphatases in control of the inflammatory response. *J Immunol* 2006;177:7497–7504. [PubMed: 17114416]
42. Lasa M, Mahtani KR, Finch A, Brewer G, Saklatvala J, Clark AR. Regulation of cyclooxygenase 2 mRNA stability by the mitogen-activated protein kinase p38 signaling cascade. *Mol Cell Biol* 2000;20:4265–4274. [PubMed: 10825190]
43. Jalonen U, Nieminen R, Vuolteenaho K, Kankaanranta H, Moilanen E. Down-regulation of tristetraprolin expression results in enhanced IL-12 and MIP-2 production and reduced MIP-3alpha synthesis in activated macrophages. *Mediators Inflamm* 2006;2006:40691. [PubMed: 17392586]

44. Yu Y, Fan J, Chen XS, Wang D, Klein-Szanto AJ, Campbell RL, et al. Genetic model of selective COX2 inhibition reveals novel heterodimer signaling. *Nat Med* 2006;12:699–704. [PubMed: 16732282]
45. Yu Y, Funk CD. A novel genetic model of selective COX-2 inhibition: comparison with COX-2 null mice. *Prostaglandins Other Lipid Mediat* 2007;82:77–84. [PubMed: 17164135]
46. Reddy ST, Herschman HR. Ligand-induced prostaglandin synthesis requires expression of the TIS10/PGS-2 prostaglandin synthase gene in murine fibroblasts and macrophages. *J Biol Chem* 1994;269:15473–15480. [PubMed: 8195190]
47. Nishida E, Hara Y, Kaneko T, Ikeda Y, Ukai T, Kato I. Bone resorption and local interleukin-1alpha and interleukin-1beta synthesis induced by *Actinobacillus actinomycetemcomitans* and *Porphyromonas gingivalis* lipopolysaccharide. *J Periodontal Res* 2001;36:1–8. [PubMed: 11246699]
48. Smith BJ, Lerner MR, Bu SY, Lucas EA, Hanas JS, Lightfoot SA, et al. Systemic bone loss and induction of coronary vessel disease in a rat model of chronic inflammation. *Bone* 2006;38:378–386. [PubMed: 16256450]
49. Rehemtulla A, Stegman LD, Cardozo SJ, Gupta S, Hall DE, Contag CH, et al. Rapid and quantitative assessment of cancer treatment response using *in vivo* bioluminescence imaging. *Neoplasia* 2000;2:491–495. [PubMed: 11228541]
50. Henson B, Li F, Coatney DD, Carey TE, Mitra RS, Kirkwood KL, et al. An orthotopic floor-of-mouth model for locoregional growth and spread of human squamous cell carcinoma. *J Oral Pathol Med* 2007;36:363–370. [PubMed: 17559499]

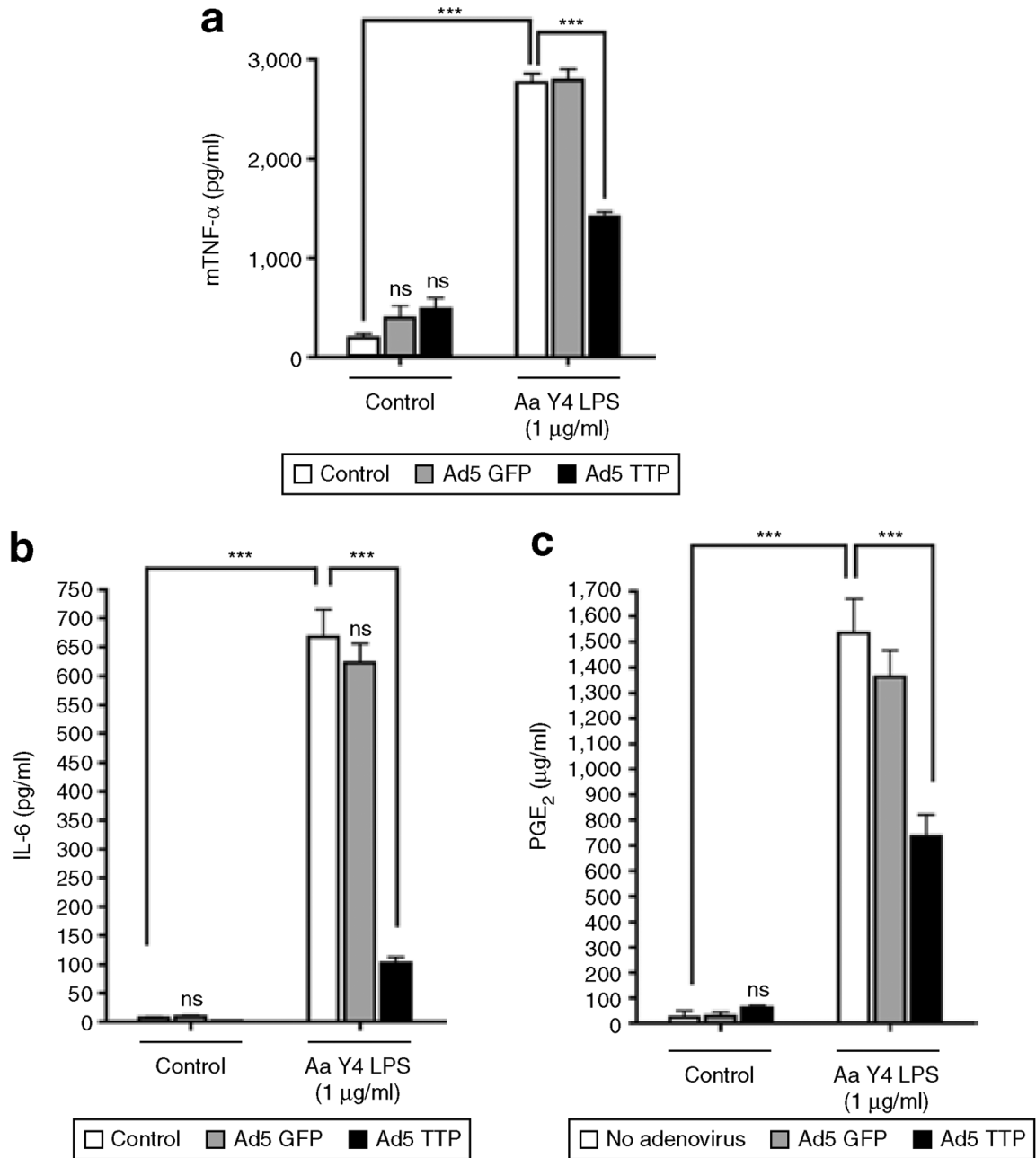


**Figure 1. Ad5-TTP potently decreases secretion of inflammatory mediators in macrophages**  
 RAW264.7 macrophages were transduced with Ad5-GFP or Ad5-TTP and stimulated with *Aggregatibacter actinomycetemcomitans* lipopolysaccharide (LPS) (1 μg/ml). Cell culture supernatants were obtained 24 hours after stimulation and subjected to enzyme-linked immunosorbent assay. Ad5-TTP reduced LPS-induced (a) tumor necrosis factor-α (TNF-α) ( $***P < 0.001$ ), (b) interleukin-6 (IL-6) ( $***P < 0.001$ ), and (c) prostaglandin (PG)<sub>2</sub> ( $***P < 0.001$ ;  $n = 3$  for each). Ad, adenovirus; GFP, green fluorescent protein; TTP, tristetraprolin.

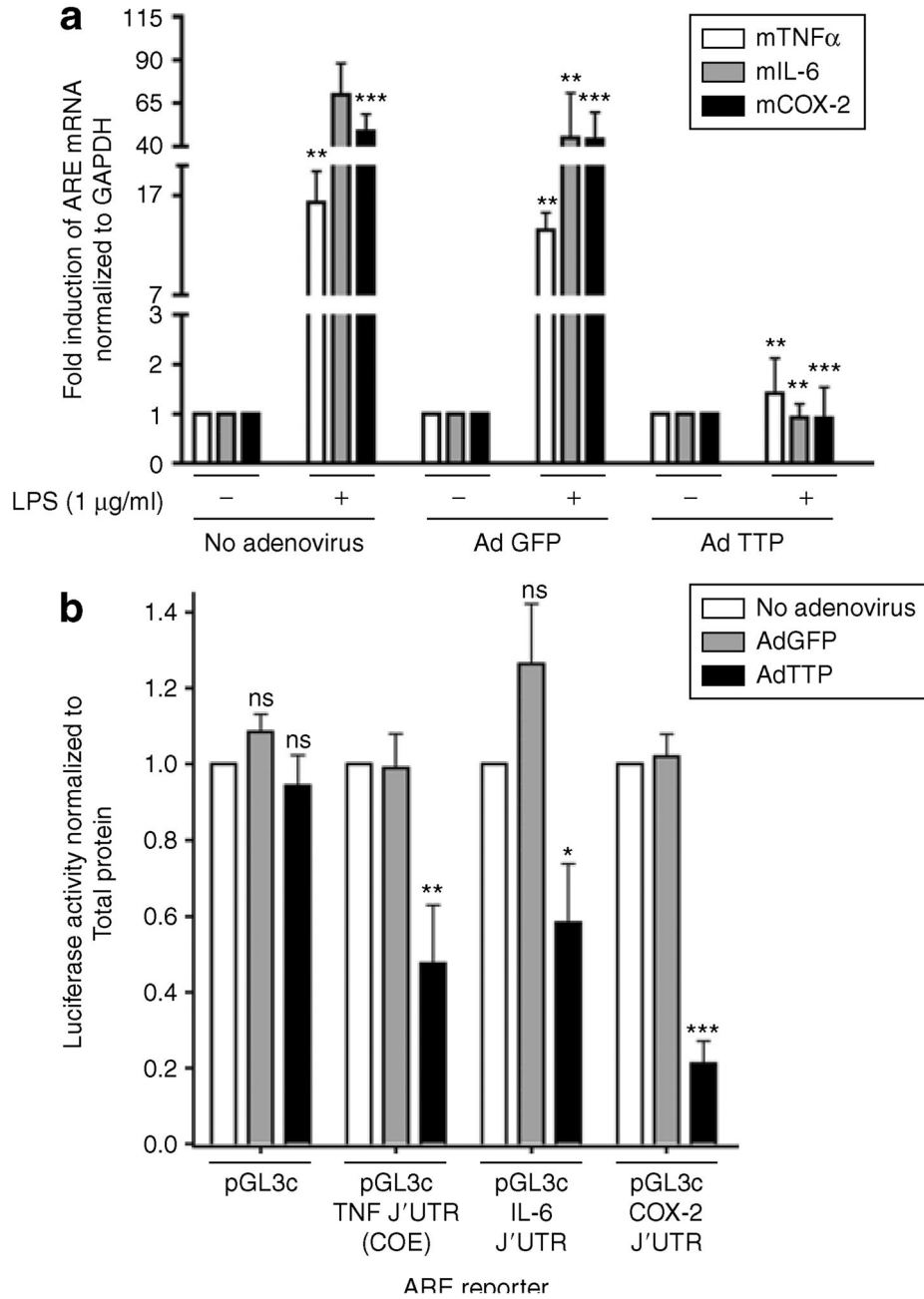


**Figure 2. Ad5-TTP specifically inhibits adenylate-uridylate-rich element (ARE)-containing transcripts**

(a) RAW264.7 macrophages were transduced with Ad5-GFP or Ad5-TTP and stimulated with *Aggregatibacter actinomycetemcomitans* lipopolysaccharide (LPS) (1 μg/ml). RNA was isolated 18 hours after stimulation and subjected to real-time reverse transcription-PCR measurement of tumor necrosis factor-α (TNF-α), interleukin-6 (IL-6), and cyclooxygenase-2 (COX-2) normalized to glyceraldehyde 3-phosphate dehydrogenase mRNA (*n* = 3 each). (b) HeLa cells were “adenofected” with luciferase reporter constructs and Ad5-TTP [75 multiplicity of infection (MOI)], Ad5-GFP (75 MOI), or no adenovirus (Ad). Luciferase reporters contained 3'-untranslated region (3'-UTR) of TNF-α, IL-6, and COX-2, or non-ARE

control pGL3-control. Luciferase activity was measured and normalized to total protein ( $n = 3$ ;  $*P < 0.05$ ,  $**P < 0.01$ ,  $***P < 0.001$ ). TTP, tristetraprolin.

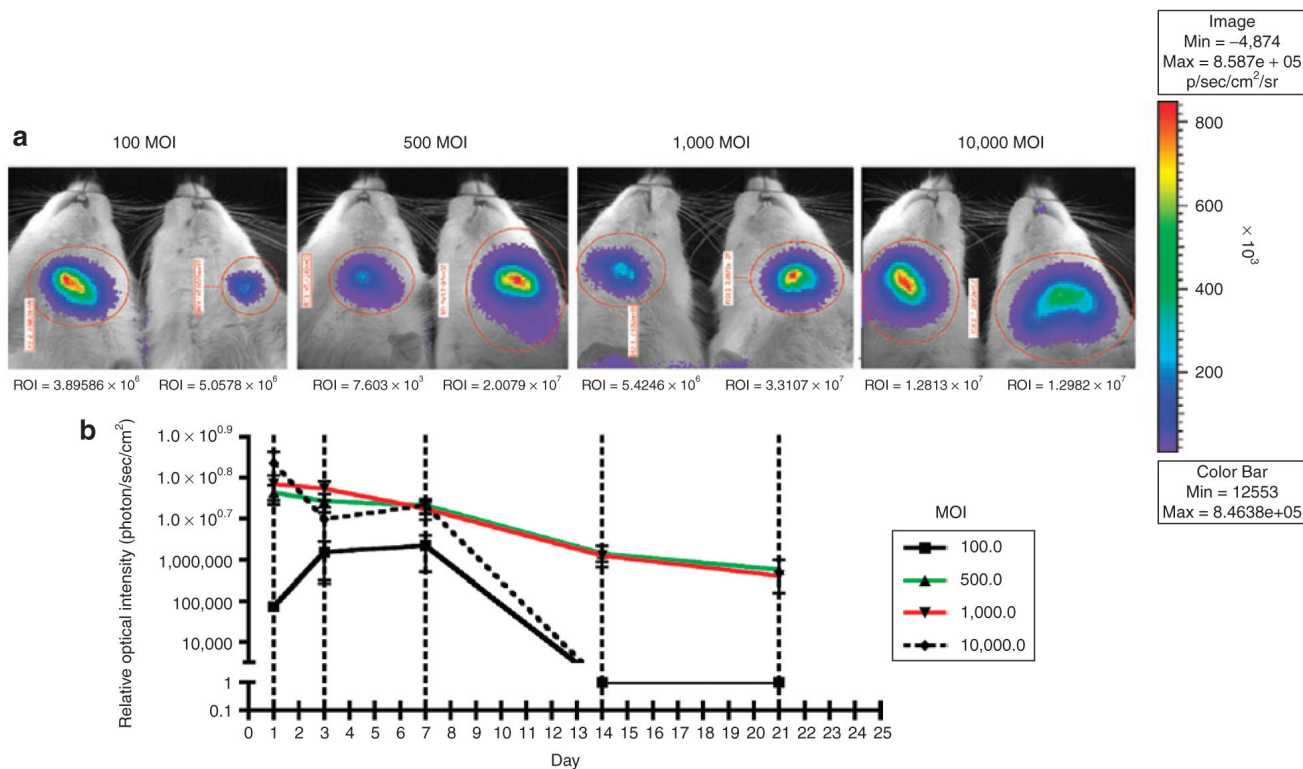


**Figure 3. Ad5-luciferase is locally expressed in rat maxillae for up to 21 days**

Rats were injected in the left maxillae with Ad5-luciferase reporter gene. Rats were the given luciferin substrate on days 1, 3, 7, 14, and 21 and *in vivo* bioluminescence was measured. (a) Representative images of rat maxillae at day 7 at indicated multiplicities of infection (MOIs) with Ad5-luciferase. (b) Graphical presentation of luciferase activity over 21 days. ( $n = 3/$  MOI). ROI, region of interest.



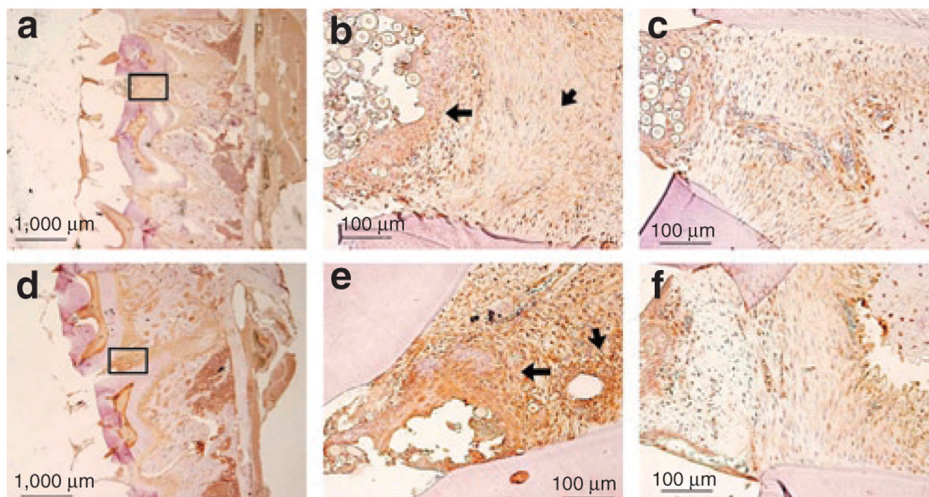


**Figure 4. Ad5-TTP is expressed in periodontal tissues throughout the experimental protocol**  
 Immunohistochemical analysis of tristetraprolin (TTP) expression in adenovirus-transduced periodontal tissues from (a) Ad5-GFP and (d) Ad5-TTP at low magnification. (b and e) Upper boxed region from a and d, respectively, at higher magnification showing Ad5-GFP-injected area between maxillary molars areas. Larger arrows indicate TTP expression in epithelial tissue and shorter arrows indicate connective tissue staining. (c and f) Lower boxed region from a and c, respectively, at higher magnification showing adjacent nontransduced periodontal tissues. Bars indicate scale. Ad, adenovirus; GFP, green fluorescent protein.

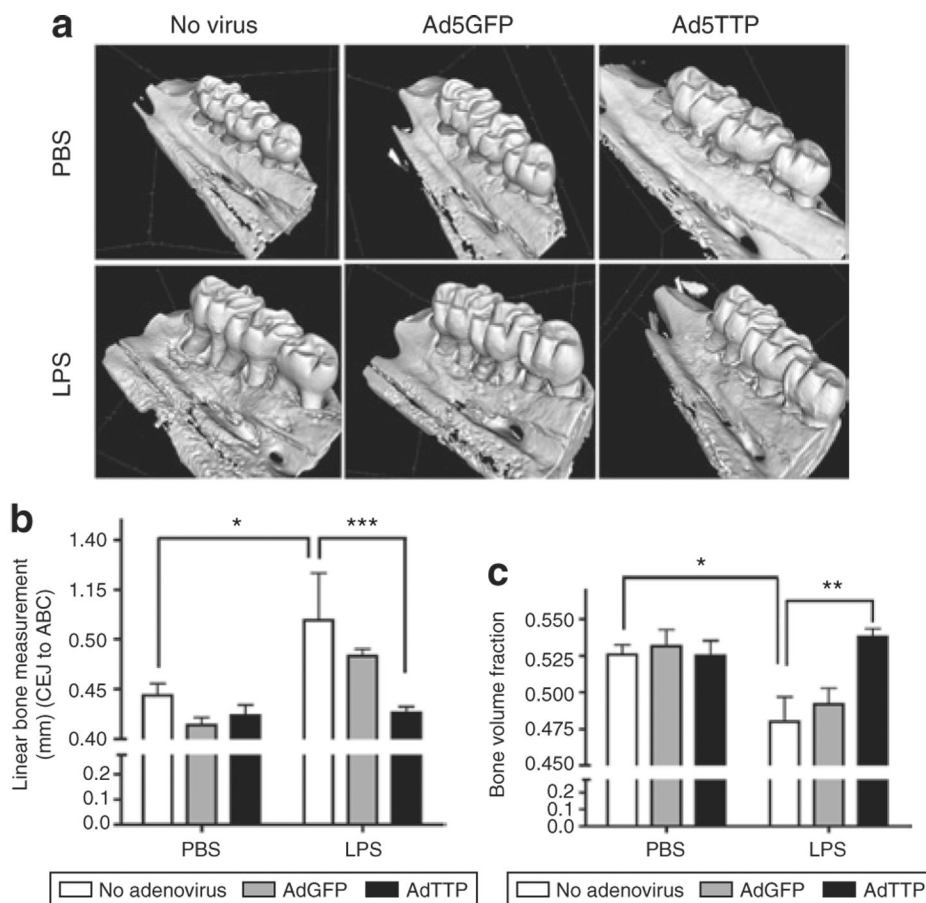


**Figure 5. Ad5-TTP protects bone in experimental periodontal disease model**

(a) Representative microcomputed tomography images of rat maxillae from indicated treatment groups. (b) Linear measurement from cemento-enamel junction (CEJ) to alveolar bone crest (ABC) ( $n = 8/\text{group}$ ;  $*P < 0.05$ ,  $**P < 0.01$ ). (c) Volumetric analysis of bone loss levels ( $n = 8/\text{group}$ ;  $*P < 0.05$ ,  $**P < 0.01$ ). Ad, adenovirus; GFP, green fluorescent protein; PBS, phosphate-buffered saline; TTP, tristetraprolin.

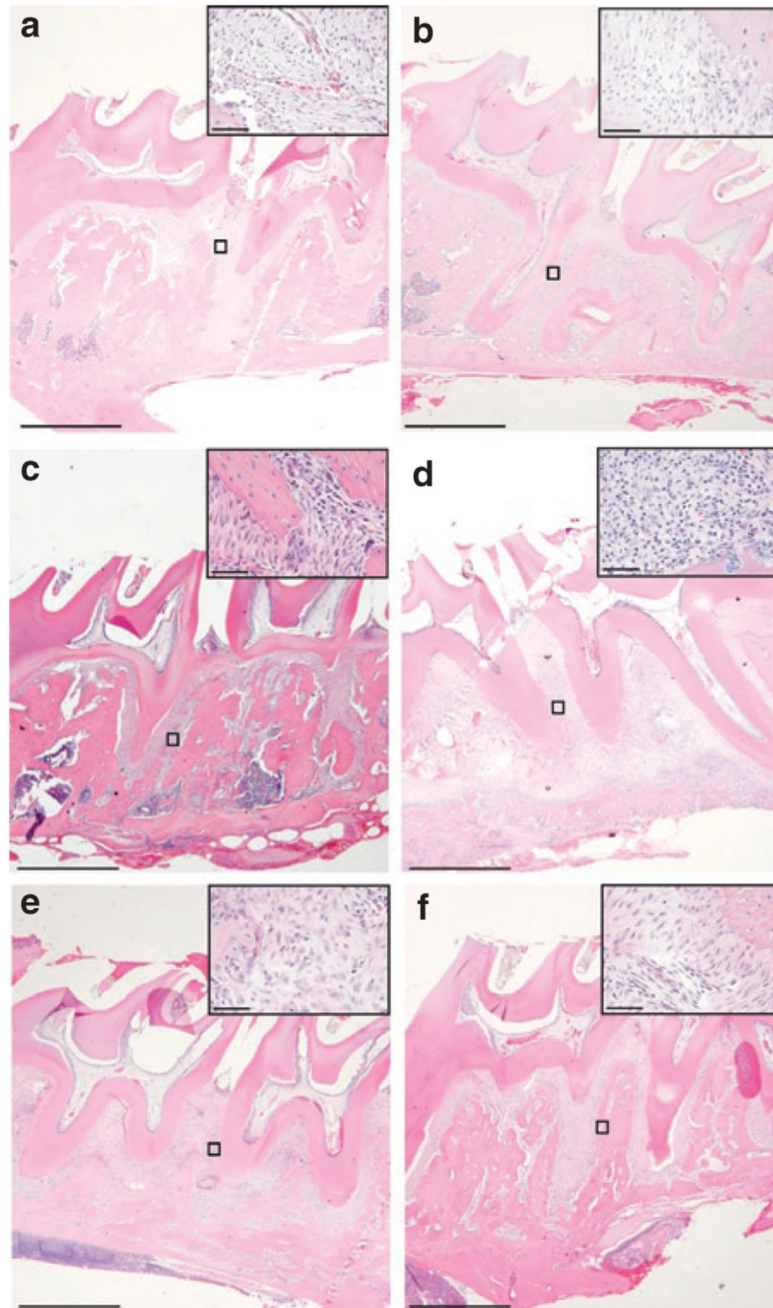


**Figure 6. Ad5-TTP reduces inflammatory infiltrate induced by *Aggregatibacter actinomycetemcomitans* lipopolysaccharide (LPS) in the area adjacent to bone loss**  
 Histological appearance of representative phosphate-buffered saline (PBS)-injected control (a), PBS + Ad5-GFP (b), PBS + Ad5-TTP (c), LPS (d), LPS + Ad5-GFP (e), LPS + Ad5-TTP (f) at low magnification (bars indicate 1,000  $\mu\text{m}$ ). Inserts of boxed areas between M1 and M2 at higher magnification (bars = 40  $\mu\text{m}$ ). Ad, adenovirus; GFP, green fluorescent protein; TTP, tristetraprolin.

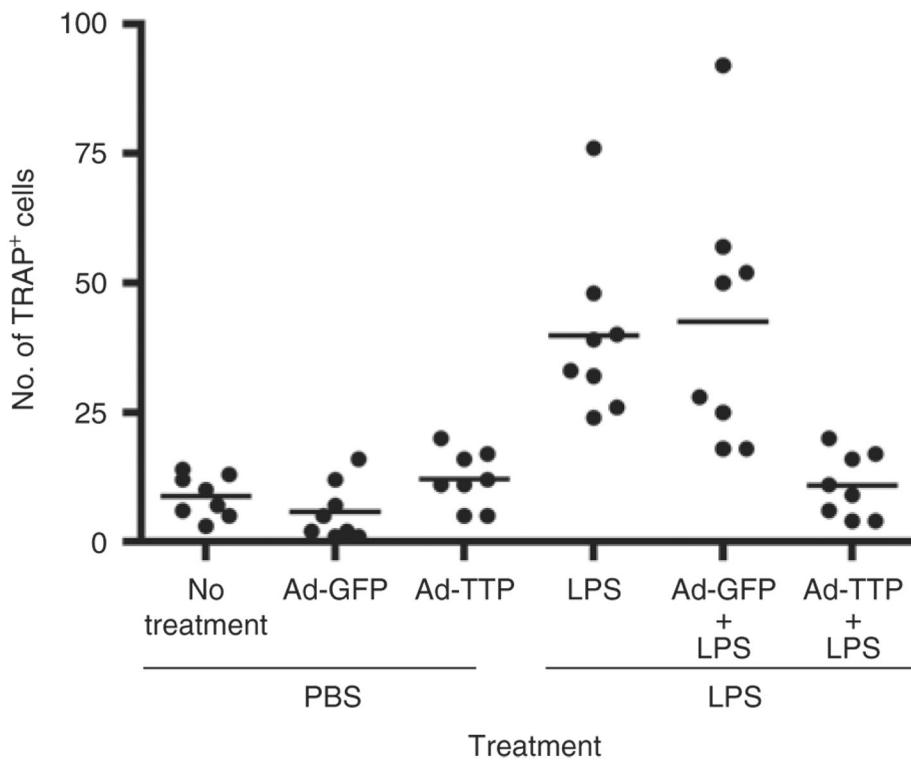


**Figure 7. Ad5-TTP reduces osteoclastogenesis in experimental bone loss model**

Tartate-resistant acid phosphatase–positive (TRAP<sup>+</sup>) cells were enumerated from similar sagittally sectioned specimens and graphically presented as a scatter plot analysis. Horizontal bar indicates mean TRAP<sup>+</sup> cell counts ( $n = 8$ ;  $***P < 0.001$ ). Ad, adenovirus; GFP, green fluorescent protein; TTP, tristetraprolin.

**Table 1**

Ad5-TT P reduces inflammatory cell infiltrate in LPS-injected animals

Group	Histological grading <sup>a</sup>
PBS	0
PBS + Ad5-GFP	5–7
PBS + Ad5-TTP	7–10
LPS	>80
LPS + Ad5-GFP	20–30
LPS + Ad5-TTP	2–3

*Abbreviations* Ad, adenovirus; GFP, green fluorescent protein; LPS, lipopolysaccharide; PBS, phosphate-buffered saline; TTP, tristetraprolin.

<sup>a</sup>Number of lymphocytes, macrophages, and neutrophils per high power field ( $\times 40$ ).